Engineering Science and Technology, an International Journal 24 (2021) 1005–1014

HOSTED BY

Contents lists available at ScienceDirect

Engineering Science and Technology, an International Journal

journal homepage: www.elsevier.com/locate/jestch

Full Length Article

Significantly improved shear, dynamic-mechanical, and mode II fracture performance of seawater aged basalt/epoxy composites: The impact of halloysite nanotube reinforcement

Hasan Ulus [a,*], Halil Burak Kaybal [b], Volkan Eskizeybek [c], Ahmet Avcı [d]

[a] Selcuk University, Huglu Vocational School, Konya, Turkey
[b] Amasya University, Department of Mechanical Engineering, Amasya, Turkey
[c] Canakkale Onsekiz Mart University, Department of Materials Science and Engineering, Çanakkale, Turkey
[d] Necmettin Erbakan University, Department of Biomedical Engineering, Konya, Turkey

ARTICLE INFO

Article history:
Received 8 November 2020
Revised 3 January 2021
Accepted 10 January 2021
Available online 12 February 2021

Keywords:
Basalt fiber (BF)
Halloysite nanotubes (HNTs)
Epoxy (EP)
Dynamic mechanical analysis (DMA)
Mode II delamination toughness (G_{IIC})
Seawater aging

ABSTRACT

The primary concern of fiber-reinforced polymers (FRPs) subjected to seawater environment is losing their initial mechanical performance since water can diffuse into the composite and deteriorates the fiber-matrix interface. Recent studies related to aging performance in the seawater environment have shown that introducing halloysite nanotubes (HNTs) into the polymer matrix offers a combination of an efficient barrier effect and an improved fiber-matrix interface. Hereupon, the principal objective of this study was to experimentally investigate the impact of HNTs on shear and mode II fracture performances of the seawater aged basalt fiber (BF) reinforced epoxy (EP) composites. After six months of aging in seawater, the findings indicated that HNTs reinforced multi-scale composites exhibited 34 and 46% higher shear strength and mode II delamination toughness compared to the neat specimens. Moreover, according to the dynamic-mechanical analysis, higher glass transition temperatures (8%) were obtained for the multi-scale composites. The reduction in mechanical performances induced by fiber-matrix interfacial degradation was also confirmed by scanning electron microscopy analysis. Chemical deterioration of the polymer matrix was explored by Raman spectroscopy to reveal the efficiency of HNTs induced barrier effect. As a result of these investigations, HNT modified BF/EP multi-scale composites were offered for future advanced engineering applications.

1. Introduction

Fiber-reinforced polymers (FRPs) have a joining of useful features such as impressive strength/weight ratios and corrosion resistance compared to traditional metallic materials. Thanks to these features, FRPs are broadly utilized in varied engineering employments such as maritime, automotive, and aviation industries, which generally serve under harsh environmental conditions [1,2]. On the other hand, it is well established that the detrimental service conditions like high-low temperature, humidity, alkalines, and ultraviolet radiation lead to severe degradations in the chemical structure and undermine mechanical performances of FRPs [3,4]. Therefore, the environmental aging of FRPs becomes a constant concern for the life-span estimation and the endurance to operational conditions [1].

Continuous seawater exposure in marine environments is a significant challenge for FRPs during their service life. Interaction with water can lead to matrix damage, fiber-matrix interface decomposition, and the development of delamination damage during service life by combining mechanisms such as hydrolysis, plasticization, and matrix swelling [5,6]. Delamination caused by environmental degradation is one of the main barriers that limit the performance and use of laminated composites in industrial applications, causing catastrophic failures [7]. Therefore, the interlaminar fracture toughness known as damage resistance against delamination between adjacent layers is of enormous significance in the improving and designing FRP composites [8]. On the other hand, the performance and damage mode of FRPs are fundamentally governed by the loading direction and the fiber reinforcement orientation. Loads perpendicular to the fiber orientation or multi-axis loading situations cause shear deformation that limits

* Corresponding author.
E-mail address: hasanulus@selcuk.edu.tr (H. Ulus).
Peer review under responsibility of Karabuk University.

https://doi.org/10.1016/j.jestch.2021.01.005

material performance [9] and causes various damages due to shear stresses [10]. So, another critical parameter to be considered in the design is the shear properties of the materials. Moreover, seawater aging also causes the plasticization due to the water molecules absorption onto the matrix. The effect would provoke increasing the distance between molecules, the expanding of molecular matrix chains, and the breaking of hydrogen bonds, resulting in a reduced glass transition temperature (Tg). Additionally, the polymer matrix oxidation-hydrolysis reactions and the fiber-matrix interface cracking caused by the absorbed water molecules also be liable for the decreased Tg [11]. Dynamic mechanical analysis (DMA) is a powerful method for sensitive and non-destructive evaluation of modal damping ratio and viscoelastic response of materials, as well as damage behavior and fiber-matrix interface properties [11]. There is little published data on the relationship between physical/chemical damage and mechanical deterioration caused by aging for FRPs. Li et al. (2019) stated that there is an exponential decline in tensile properties and Tg with prolonging aging time in the marine environment in their studies on the static and dynamic mechanical performance of carbon/epoxy composites [12]. Panaitescu et al. (2019), as a result of their research on thermomechanical properties of glass fiber reinforced polyurethane composites under accelerated aging environment, deduced that while water absorption causes reversible aging of the matrix material, it leads an irreversible deterioration of the composite [1]. Mlyniec et al. (2014) explained the effect of aging on damping behavior in composite structures with the modal damping ratio. They emphasized that the durability of fiber, matrix and fiber-matrix interfacial properties should be taken into account to procure long-time damping performance in carbon fiber reinforced EP composites exposed to DMA damping vibrations [13]. On the other side, although the researches about the aging effect on the interlaminar shear strength (ILSS) of FRPs are included in the literature, the influence of aging on the v-notched rail shear properties has been examined by only a few researchers. Costa et al. (2010) found a decrease in shear strength when they evaluated shear behavior with the Iosipescu shear test method of glass fiber reinforced polyphenylene sulfide composites after aging [14]. Figliolini et al. (2013) stated that the absorption of seawater slightly increased the ductility of vinyl ester resin samples and reduced the notch sensitivity, causing an increase in shear strength [15].

Recently, basalt fiber reinforced polymers (BFRPs) are introduced as a substitute for glass and carbon composites in marine applications by courtesy of their high strength, low manufacturing cost, and distinguished corrosion behaviors [16]. The increasing interest in BFRP composites has triggered studies investigating its behavior under different environmental conditions [17]. Several researchers have shown that modification of the EP matrix by adding nanoreinforcements is promising for improving the mechanical performance of BFRP composites [18–20]. Nanoreinforcements trigger the growth of cross-linked amine networks in the curing reaction of epoxies, providing an enhanced fiber-matrix interfacial bonding. Therefore, EP matrix modification, which performed with the addition of the nanoparticles, is one of the effective ways to increase mechanical performance in a hydrothermal condition [21]. Halloysite nanotubes (HNTs) have lately been the issue of study as a novel and inexpensive nanoreinforcements to ameliorate the mechanical performance of polymers and especially epoxies [22–24]. In our previous studies, we have also been reported that the matrix modification performed with low percentages of HNTs adding into the EP improves seawater aging durability of BFRPs [5,6].

Although there are several studies on the mechanical performance of HNT modified composites, what is not yet clear is the impact of HNTs modification on seawater aging of basalt fiber (BF) reinforced epoxy (EP) composites. This study presented here is one of the first investigations to focus specifically on the influence of HNTs modification on the delamination behavior of long-term seawater aged BF/EP composites under mode-II loading with ENF tests and shear properties with V-notched rail shear tests. Additionally, the DMA technique was utilized to characterize thermomechanical properties and to confirm matrix and fiber-matrix interface behavior. Finally, the impact of HNTs modification and aging on the chemical damages were systematically explored using Raman analysis. The results reveal that the proposed epoxy matrix modification may be a promising strategy for the seawater durability of BF/EP composites. This method can be widely used as a simple and economical way of improving the performance of BFRP composites

2. Experimental

2.1. Materials

Basalt plain woven fabrics (300 g/m^2 areal density and 0.45 mm average thickness) were kindly supplied by Tila Kompozit. MGS epoxy resin (L-160) and MGS hardener (H-160) were obtained from DOST Chemical Industrial Raw Materials Industry. Halloysite nanotubes (20–150 nm in diameter and 100–600 nm in length) were supplied by Eczacibasi Group ESAN Company. All reagents were of analytical grade and utilized without more purification.

2.2. Fabrication of multi-scale composites

The produced HNTs reinforced EP resins (by including 2 wt% HNT) were prepared considering by the determined optimal nanoparticle ratio based on our previous studies [5,6]. In the former case, required amounts of the nanoreinforcements were dispensed in acetone to achieve uniform distribution, and in the latter case, the epoxy was poured into the HNT-acetone blending. The mixture was sonicated by probe ultrasonicator (for 1 h at 20 kHz) to obtain a homogeneous suspension under an ice bath (~60 °C suspension temperature). Besides, the matrix material of neat composites was also prepared following the same procedure (only without HNT) as multi-scale composites. Following, the mixture was warmed up in a vacuum furnace to evaporate the acetone (for 12 h at 70 °C). At this stage, attention should be paid to cool the mixture to room temperature to prevent an uncontrolled curing reaction. Finally, the amine hardener was mechanically mixed (for 5 min) with the resin under the stoichiometric ratio of 100:25 (for 100 g epoxy 25 g of hardener), as per manufacturer's directions and the final mixture was degassed for 15 min, at 35 °C. The Vacuum Assisted Resin Transfer Molding (VARTM) method was used to manufacture BFRP composites because of its advantages, such as large-scale manufacturing and low production costs. After the curing process (for 1 h, at 70 °C, and for 4 h, at 120 °C), composite panels were cut to appropriate sizes, and test coupons were formed. The composite specimens were then aged in a seawater bath at room temperature for 3–6 months. The aging of samples was performed by immersing into prepared artificial seawater according to ASTM-D1141 by mixing the sea salt (6 wt%) and distilled water [5,6].

2.3. Mechanical tests

The performed tests in the study are conceptually illustrated in Fig. 1. V-notched rail shear testing was executed to assess the impact of seawater aging on the composites' in-plane shear performances. This methodology ensures the measure of the shear properties by compressing the ends of a V-notched sample between a pair of shear test apparatus. In-plane V-notched rail shear tests

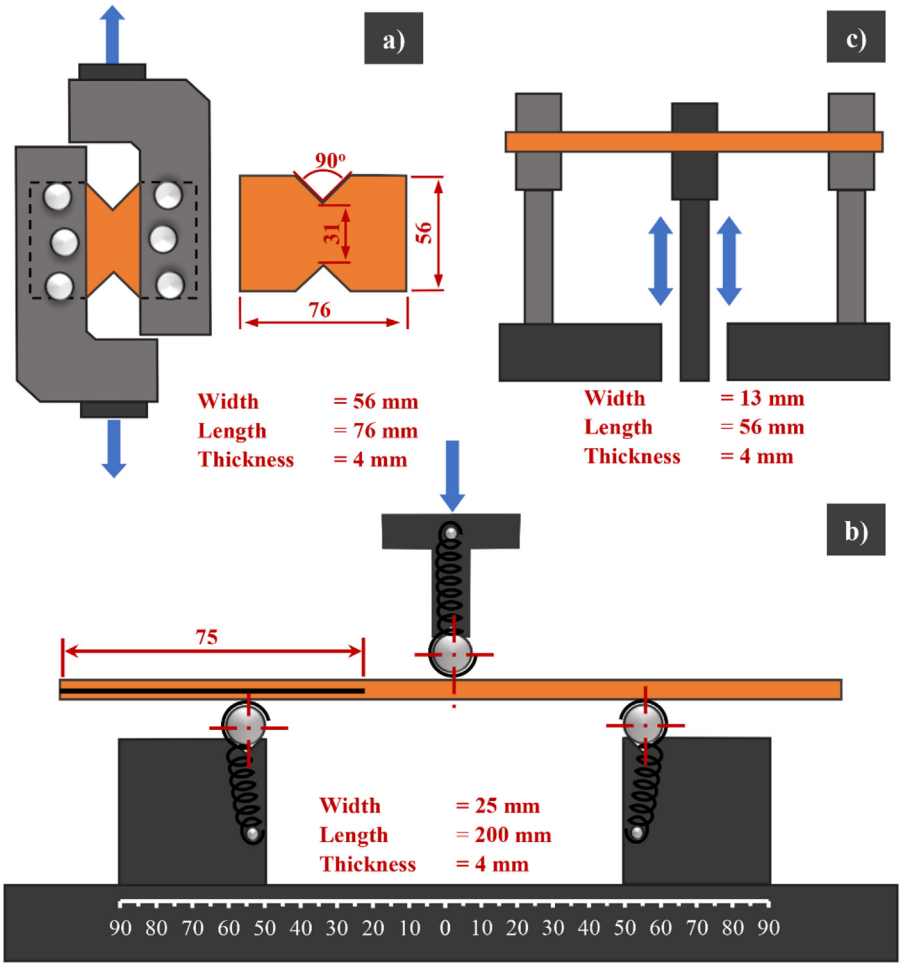

Fig. 1. Schematic illustrations of the tests: a) V-notched rail shear test, b) End notched flexural (ENF) test c) Dynamic mechanical analyses (DMA).

were implemented on an Instron 8801 with 2 mm/min cross-head speed as per ASTM D7078M – 19.

End notched flexure (ENF) tests were performed to assess II delamination toughness according to ASTM D7905-14 standard. At least five specimens were tested with the dimensions of 180x25x4 mm^3. A teflon film (with a length of 75 mm) was inserted at the midplane to form a pre-crack in the ENF test laminates during fibers fabric stacking. Mode II interlaminar fracture tests were carried out under 1.5 mm/min cross-head speed via Shimadzu AGS-X instrument, and the effective span was adjusted as 80 mm. One side of the ENF samples was painted with a correction pen to track crack propagation accurately during the delamination easily. The tests were recorded by a digital camera to measure crack length later on.

The DMA analysis was conducted on Perkin Elmer DMA 8000 to investigate the impact of the plasticization effect of seawater aging on the basalt-epoxy interface. Moreover, to focus on the impact of aging on the polymer, bulk epoxy samples were also analyzed, which manufactured using liquid composite molding (LCM) process. Therefore, two kinds of specimens were employed, which were produced as laminated (fiber reinforced) specimens and bulk epoxy (without fiber) specimens in these analyses. The same curing process was applied for bulk epoxy specimens. The tests were performed on rectangular specimens of 56x13x4 mm^3 prepared according to ASTM D7028-07. DMA tests were conducted in 3P bending mode at 1 Hz fixed oscillation frequency while the temperature was increased from 0 to 200 °C with a 5 °C/min heating rate.

2.4. Characterizations

Surveying of scanning electron microscopy (SEM) was realized on the damaged ENF samples' delamination surfaces by A Zeiss Evo LS 10. The fracture surfaces were visualized to understand HNTs related toughness mechanisms and/or impact of seawater aging on damage mechanisms. The SEM specimens were covered with 4 nm thickness gold sputter coating and imaged at 20 kV electron beam acceleration voltage. Raman spectroscopy was conducted with WITEC Alpha 300 Confocal Raman system with a 532 nm laser irradiation to reveal the seawater aging effect on the epoxy structure. Raman examinations were performed with a scan range of 3785–200 cm^{-1} at a resolution of 4 cm^{-1}.

3. Results and discussion

3.1. V-notched rail shear test

The typical load–displacement curves are shown in Fig. 2 for V-notched rail shear tests. Before seawater aging, for neat samples, it is observed that the shear force suddenly falls after arriving at the peak value. However, it can be seen that the load drops gradually after reaching the peak point in the case of the multi-scale composite samples. The gradual decline indicates an increased load transfer efficiency from the matrix to the fibers or vice versa, which suggests improved fiber-matrix interface interaction with the HNTs modification [25]. After seawater aging, a shoulder forms with increasing shear strain beyond the maximum shear stress

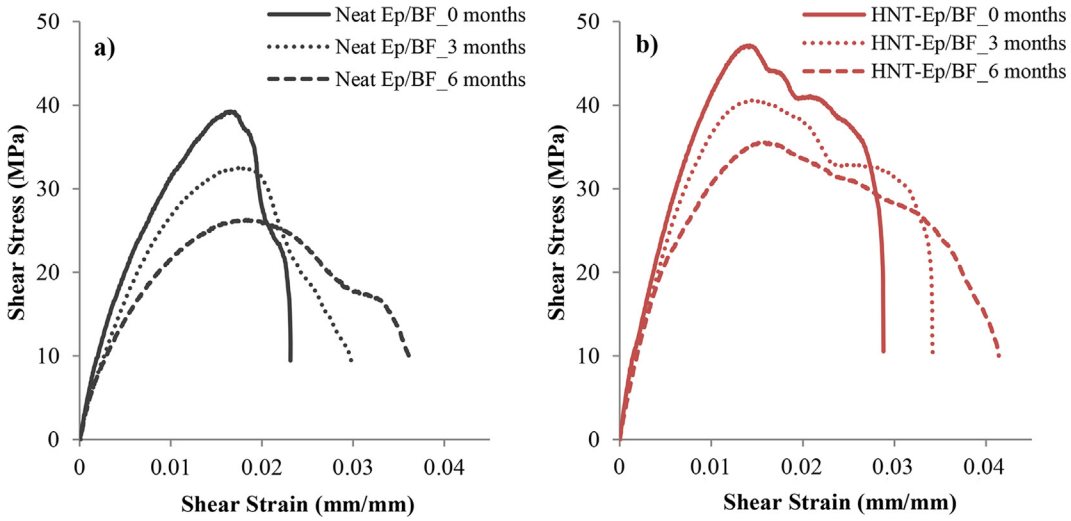

Fig. 2. Typical stress–strain curves of v-notched rail shear test specimens: a) neat BF/EP composites, b) HNT modified BF/EP composites.

indicating the matrix plasticization due to the absorbed water into the matrix. On the other hand, it is noticed that gradual load drops observed for the multi-scale composites before aging slightly disappear due to the deterioration of fiber-matrix interface.

As compiled in Table 1, it is evident that the matrix modification by HNTs significantly improves the shear properties. Before aging, the shear strengths of neat epoxy and multi-scale composites are calculated as 39.25 and 47.16 MPa, respectively. It is clear that the increase in shear strength is achieved by HNTs related toughness mechanisms such as crack deflection, crack pinning, and pull-out [5,6]. On the other hand, the obtained shear strengths decline for both neat and multi-scale composites after 6 months of seawater aging (26.28 and 35.10 MPa, respectively). However, it is noted that the multi-scale composites exhibit significantly higher shear strength up to 33.5% compared to the neat samples. Similarly, to evaluate the effectiveness of HNT addition modification on shear modulus, multi-scale composites represent 19% higher shear modulus compared to neat composites, and the increase reaches up to 45% after 6-months seawater aging. Alamri and Low reported that high aspect ratio HNTs ensure excellent barrier properties by forming a tortuosity leakage path for water diffusion into the epoxy [23]. On the other hand, the enhanced load transfer effectiveness at the fiber-matrix interface can occur as another possible strengthening mechanism [26]. As we reported in our previous studies, this significantly enhanced seawater aging performance has been attributed to the restricted water diffusion mechanism rather than the toughness mechanisms provided by HNTs [5,6].

It can be noticed from Table 1 that the shear failure strain increases from 0.023 to 0.028 mm/mm (21.7% higher than the neat composites) with the HNTs modification. Moreover, as the aging time is increased to 6 months, gradual increases in shear strain are observed, which is another indication of the plasticization effect. It is obtained that the seawater immersion leads to deforming at higher shear strains as 56.5 and 46.4% for neat and multi-scale composites, respectively. Interestingly, lower strain values are obtained for the multi-scale composites compared to that of the neat composites. This result is primarily influenced by the barrier effect on the water diffusion realized with the introduction of HNTs into the epoxy retarding matrix plasticization during seawater aging [23].

3.2. Mode-II interlaminar fracture test

The ENF samples are exposed to shear loading near the teflon film, and initiation cracks progressing in front of the crack tip are provided to perform mode-II fracture toughness tests. As the applied load increases, microcracks coalescence, and crack propagation is initiated. Immediately after reaching the peak load value, the load drops suddenly. This maximum load value is used to calculate the critical mode-II interlaminar fracture toughness (G_{IIC}). Fig. 3 shows force–displacement curves for the neat and multi-scale composites. The aged specimens generally have exhibited lower peak forces and higher compliances due to the plasticization effect compared with that for the dry specimens [27]. In general, the load rises with a linear inclination till it arrives at a critic value corresponding to the beginning of crack propagation. Sudden load drops caused by unstable crack propagation are obtained for the neat samples while the formation of a plateau region is explicit for multi-scale composites indicating more stable crack propagation. Friction between delaminated layers is responsible mechanisms attributed to mod-II delamination toughness values [28]. EP modification with HNTs renders the matrix region tougher. During the effect of the shear load, multi-scale composites better resist the delamination thanks to improved friction between the interlaminar layers and improved interface features. Thus, the modified

Table 1
Shear test results of BF/EP composites.

	Aging Time (months)	Stress (MPa)	Decrease (%)	Strain (mm/mm)	Shear modulus (GPa)	Decrease (%)
Neat Ep/BF	0	39.25		0.023	3.78	
	3	32.61	16.92	0.029	3.09	18.12
	6	26.28	33.049	0.036	2.45	35.16
HNT-Ep/BF	0	47.16		0.028	4.51	
	3	40.59	13.92	0.034	3.96	12.36
	6	35.10	25.56	0.041	3.56	21.08

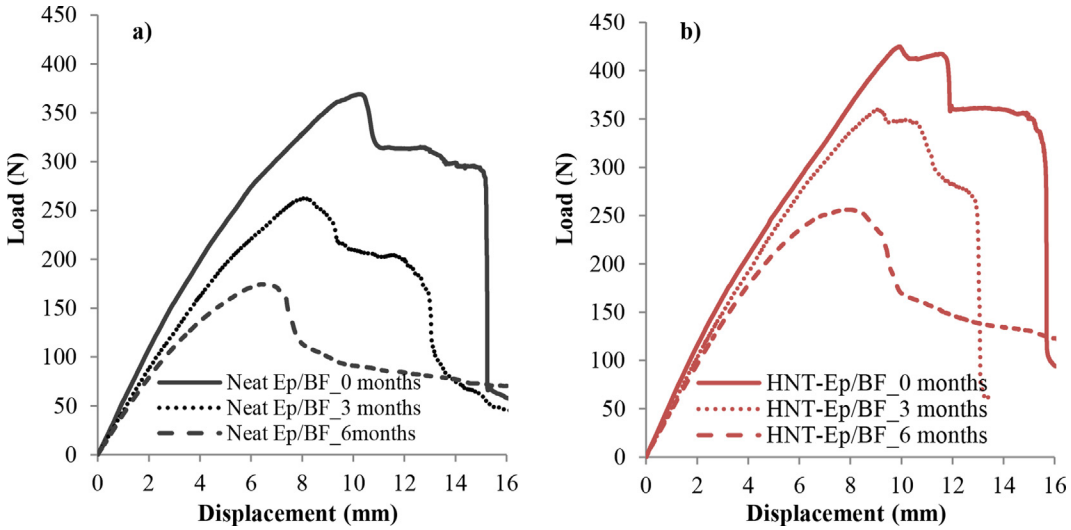

Fig. 3. Typical load–displacement curves of ENF specimens: a) neat composites, b) multi-scale composites.

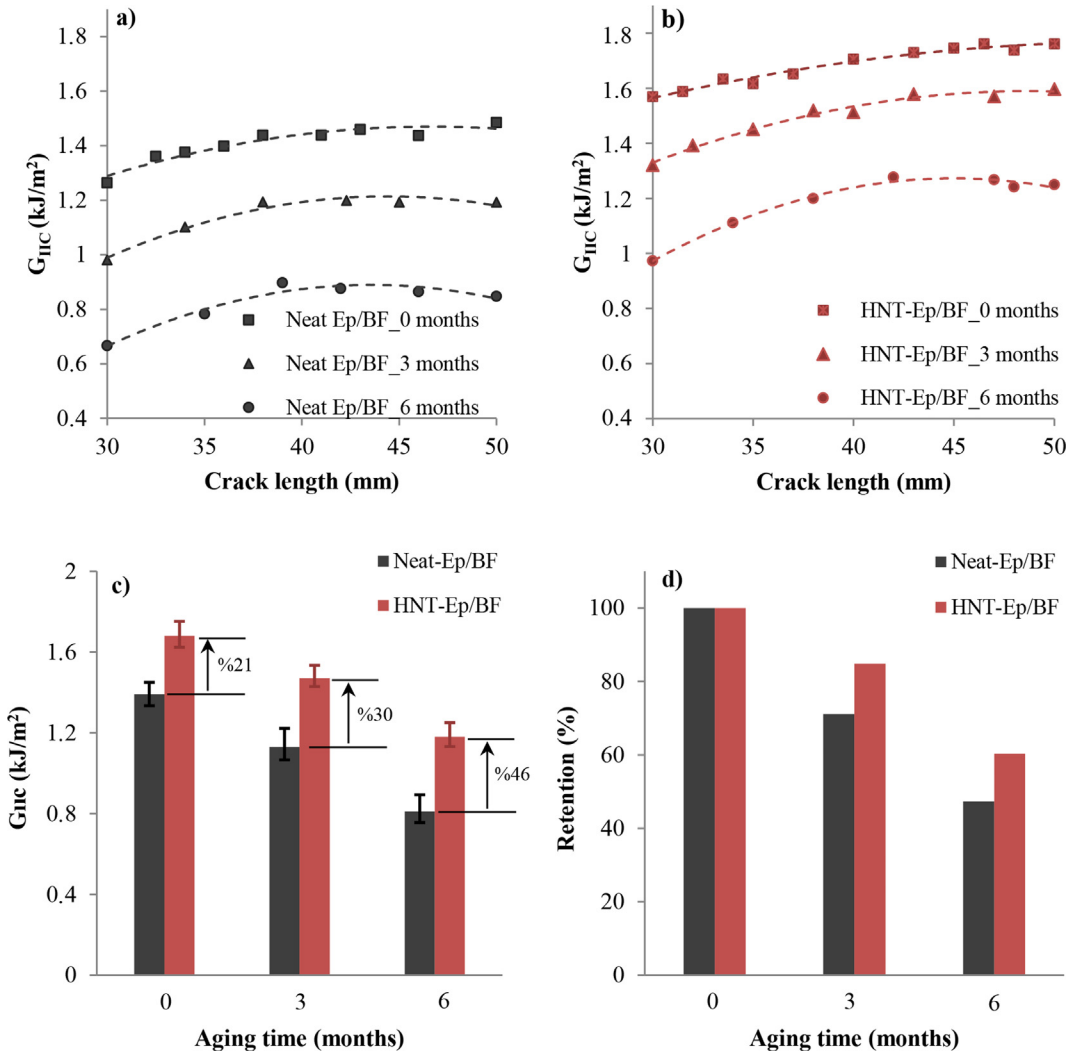

Fig. 4. ENF test results: a and b) Representative R-curves, c) G_{IIC} values as a function of seawater immersion duration, d) G_{IIC} retention (%) as a function of seawater immersion duration.

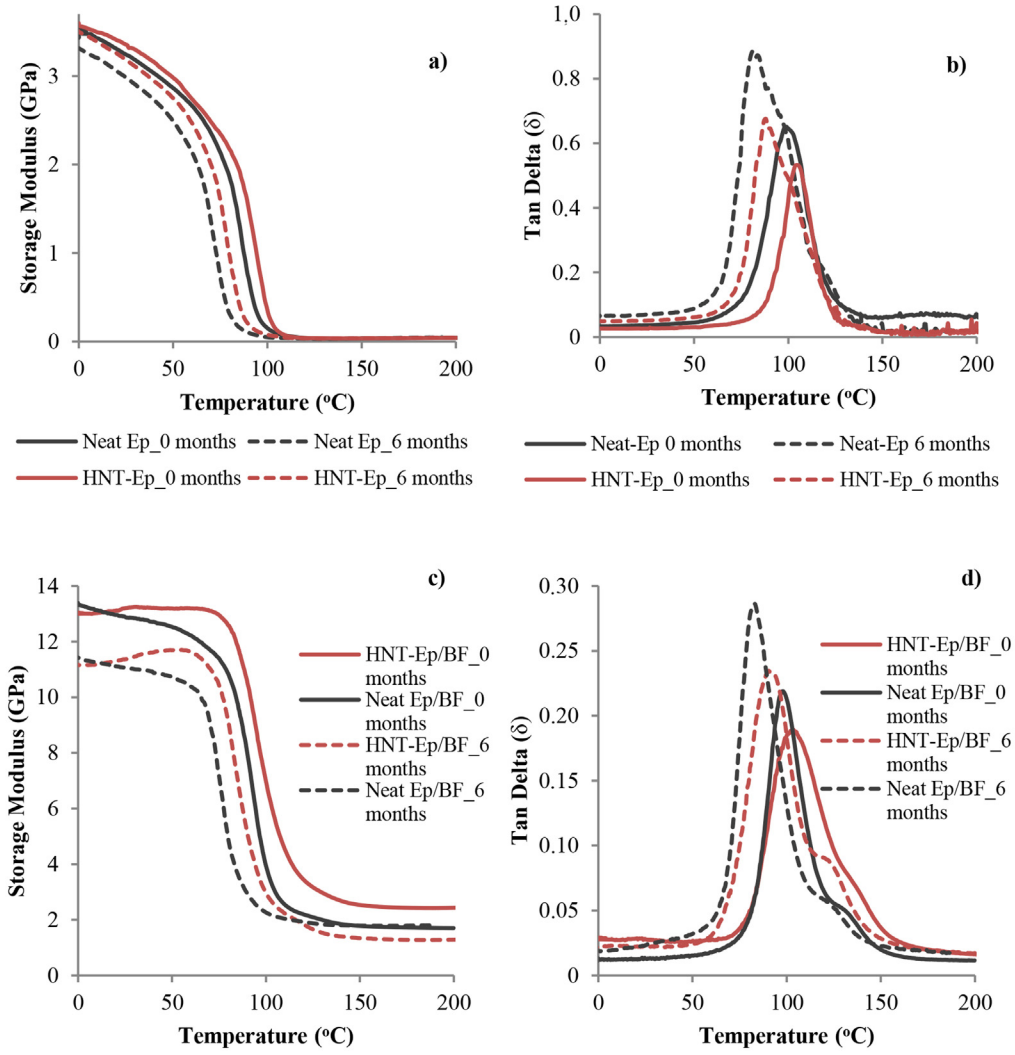

Fig. 5. (a and b) storage modulus and (c and d) tan delta alteration depending on the temperature.

samples' delamination damage occurs at higher loads than the neat [28]. It has been previously reported that the fiber-matrix interface and the interlaminar bonding are improved with EP matrix modification by adding HNTs [5,6,29]. Moreover, according to some studies, HNTs lead to covalent cross-linking density increment between the nanotube and the EP matrix which is held liable for the substantially enhanced performance [29,30]. Similarly, the increased crack growth resistance attributed to the significant impact of fiber-matrix interface interactions developed by the HNTs addition into the matrix [6,31].

The resistance curves (R-curves) are obtained by the compliance calibration method and presented in Fig. 4(a and b). While R curves show similar trends for the neat and the multi-scale composites, it is clearly seen that the neat composite exhibits relatively lower delamination resistance compared to the BF/EP multi-scale composites. Averaged G_{IIc} values, including standard deviations and changes in percentages of seawater aged samples, are summarized in Fig. 4c and d. Note that G_{IIC}values decrease with the prolonged seawater aging time from 1.39 to 0.81 kJ/m^2 after 6 months for the neat BF/EP composites. Similarly, average G_{IIC} values of the multi-scale composites exhibit a lower reduction from 1.68 to 1.18 kJ/m^2. After 6-months of seawater aging, G_{IIC} delamination toughness of the neat and the multi-scale composites was decreased by about 28 and 20%, respectively. Besides, thanks to the HNTs modification, the difference of obtained fracture toughness values between neat and multi-scale composites reaches up to 45.6% due to the higher degradation rates of the neat matrix. The impact of aging on the mode II fracture behavior is a resultant of two rival effects. One of these, the plasticization effect caused by water absorption, reduce brittleness, and increases the fracture toughness. On the other hand, it weakens the fiber-matrix bond at the same time which results in impairing the fracture resistance [27]. The results reveal that damages the bonding between the fiber and matrix occurs more predominantly.

All the representative experimental R-curves tend to increase with crack propagation. The increase of G_{IIC} values are due to the interior irregularity in the woven fiber-reinforced composites, and the BF above and below the midplane tended to bridge the delamination as crack grew [32]. It can be seen from the dry specimens, as the delamination propagates, the R-curves exhibit a rise in the initial stages of crack growth and eventually reach the relatively steady-state (seen as plateau region). On the other hand, in the case of aging in seawater, the R-curve rises, however, reaches a steady-state region less stable than the dry specimens [33]. This can be explained by a weakening of fiber-matrix bonding, which can be attributed impact of seawater aging. Moreover, it is noticed

that crack propagation occurs in seawater aged specimens at large intervals; namely, the delamination crack progresses in bigger steps. This can be attributed to the fact that low mode-II delamination toughness (G_{IIC}) of seawater aged composites.

3.3. Dynamic mechanical analysis

The evolution of the storage modulus (E) based on the temperature at constant frequency is seen in Fig. 5(a–c). While an exponential decrease in E for the bulk epoxy samples (without fiber) with extended aging time is observed, the curves of the BF/EP samples appear to form two different regions as a glassy region (above Tg) and a rubbery region (below Tg). In the glassy are region, specimens display high storage modules due to components that are highly immobile and closed-packed. However, as the temperature rises, the components turn into more mobile, stiffness, and storage modulus reduce observed due to the loss of close packing arrangement. It is clear that the multi-scale composite samples represent higher storage modules due to the fact that HNTs provide a better fiber-matrix interaction at the interface, causing a fall in the molecular mobility of the molecular chains [26,34,35]. Similarly, it is possible to associate the decrease of storage modulus values after aging with the weakening of the fiber-matrix interface bond by increasing the chain mobility [35]. Therefore, the investigation of damping (tanδ) change is also a suitable strategy for the quantitative characterization of the damage caused by aging in materials. If the fiber-matrix interfacial bonding is adequate, damping decreases due to the reduced polymer chain mobility [12]. In Fig. 5(b–d), the dumping value increase can be seen that can be associated with the fiber-matrix interfacial deterioration with the prolonging aging time. In addition, Tg can be detected from the temperature values in which the peak value is reached in the damping curves. Besides, the influence of the aging duration on the Tg value of samples can be compared in Fig. 5(b–d). The Tg values of the dry-neat and HNT modified epoxy bulk specimens (without fiber) were obtained as 98.9 and 103.5 °C, respectively. After 6 months of aging in seawater, the Tg of bulk samples degraded to 81.6 °C for the neat epoxy and 88.15 °C for HNT modified epoxy specimens with a reduction of 17.45 and 14.90%, respectively. The Tg values for the neat and multi-scale (fiber reinforced) dry specimens were observed to be 99.3 and 104.2 °C, respectively. After 6 months of aging in seawater, the Tg of samples degraded to 83.2 °C for neat BF/EP and 89.4 °C for multi-scale BF/EP specimens with a reduction of 16.14 and 14.18%, respectively.

3.4. SEM analysis

Fracture surfaces (near the crack-tip) were observed utilizing SEM (Fig. 6a–f) to observe the impact of epoxy modification and seawater aging on the interlaminar fracture mechanisms. Fig. 6a–c represents neat BF/EP composite and Fig. 6d–f multi-scale composite samples. In general, the SEM micrographs broadly demonstrate that there is a rise in the surface roughness due to the addition of HNTs (Fig. 6a–d). Similar roughness increase observed here as in our previous studies suggests that there are various toughening mechanisms liable for improved mechanical performance, such as HNTs pull-out, crack pinning, and crack deflection [5,6]. Additionally, the influence of seawater aging can be noticed by careful examinations. The delaminated fracture surface of unaged composites generally displays more fragment debris between the fiber matrix regions, which refers to the brittle feature of highly cross-linked epoxy [36]. However, the fractured surface of seawater aged composites displays comparatively smooth texture due to the water molecules penetrate the matrix and weakened fiber-matrix interfacial bonding. As a result, fibers readily pull out from the weakened fiber-matrix interface. The diminishment of matrix fragment on the fibers and delaminated surfaces illustrates the increment in the ductility induced by the plasticization effect. On the other hand, when the epoxy is modified with HNTs, the diffusion of water molecules into the epoxy matrix is restricted due to the efficient barrier effect of HNTs. Therefore, the fracture surface roughness, which is mainly governed by the fiber pull-out mechanism, is reduced for the multi-scale composite samples compared to neat specimens. Thus, the enhancement of

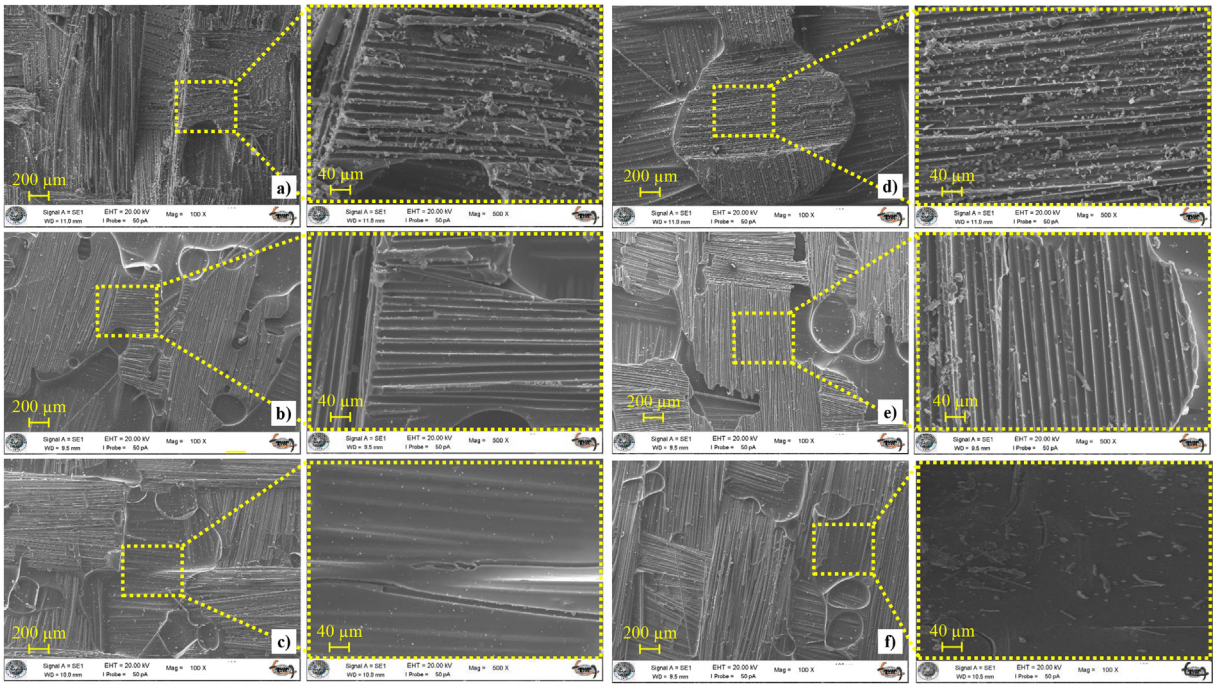

Fig. 6. SEM images of the ENF specimens' delamination surfaces: a) neat unaged composite, b) 3 months aged neat composite, c) 6 months aged neat composite, d) unaged multi-scale composite, e) 3 months aged multi-scale composite, f) 6 months aged multi-scale composite.

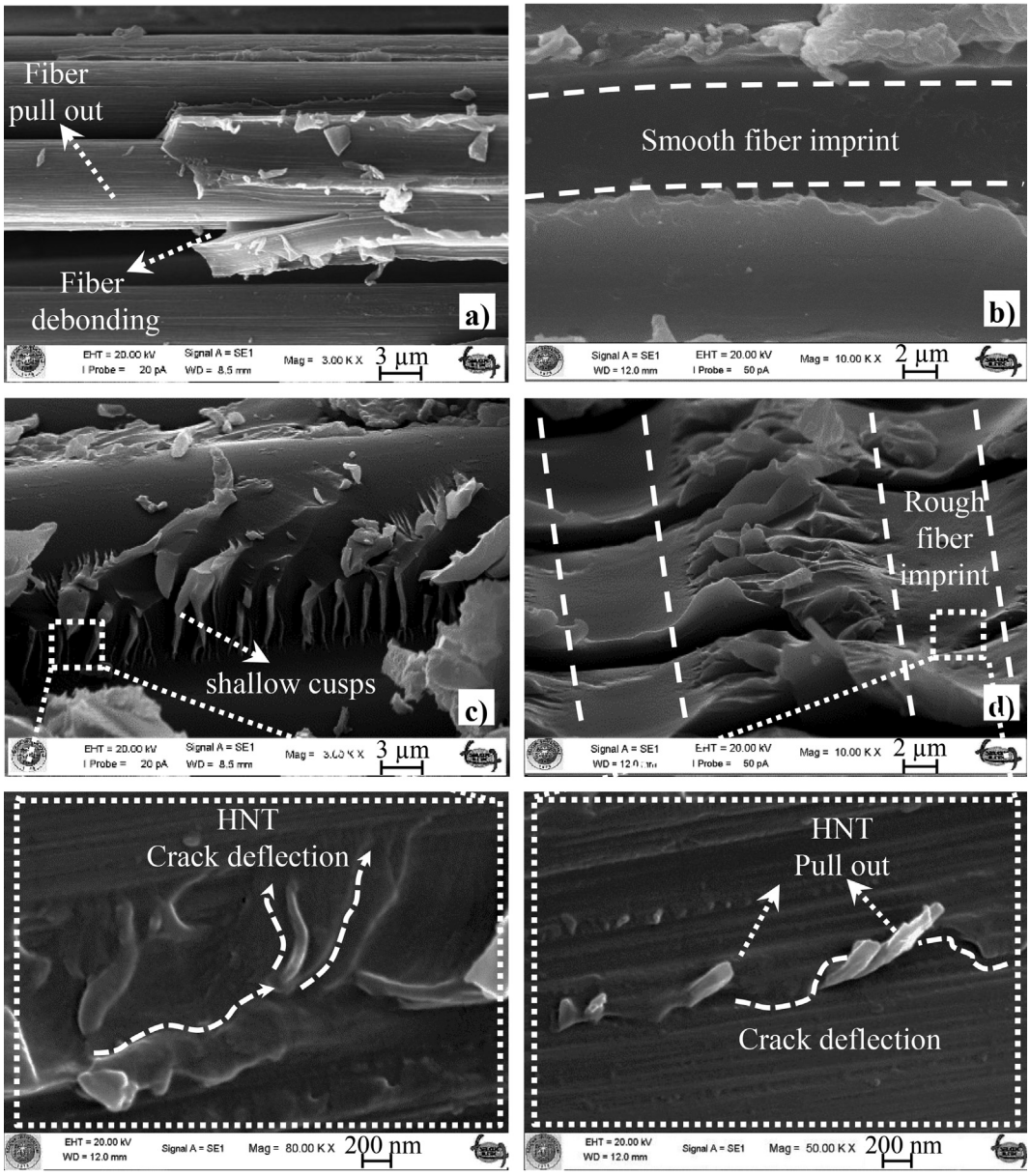

Fig. 7. SEM images of the un-aged specimens: a and b) neat composites, c and d) multi-scale composites.

mechanical performances for multi-scale composites is not only dependent on the additional nano-scale toughness mechanisms but also the suppression of water absorption by a restricted diffusion mechanism.

SEM images at higher magnifications taken from unaged samples to investigate the toughening mechanisms of HNT nanoreinforcements are seen in Fig. 7. Fibers pull out, and fiber-matrix debonding damages caused by weak fiber-matrix interaction are clearly seen in Fig. 7a for the neat epoxy. Shallow cup formations (proof of the excellent number of shallow cusps on the fiber edges with good bonding) with the HNT addition are seen in Fig. 7c. The formation of resin residues around the fiber is due to the progression of a crack close to the interface and changing direction when it encounters with nanoparticles (Fig. 7c and d). Thus, the crack cannot progress in the fiber-matrix interface with an unsteady growth characteristic, and fiber imprints are formed at the interface, indicating increased fracture resistance. In addition, the presence of nanoparticles in BF/EP composites promotes mechanical locking between crack interfaces. Besides, as a result of crack deflection, extra energy is needed to crack progressing in structure. Thus, mechanisms such as crack deflection and HNT's pull-out increase the strength values [28].

3.5. Raman analysis

Raman analysis was also conducted to determine chemical destruction of the matrix and fiber-matrix interface. Water containing OH^- ions react with the hydrophilic groups in the epoxy networks and binds to the epoxy structure (with van der Waals and hydrogen bonds) and consequently affects the absorption of radiation. Raman spectra taken from the delamination surfaces of tested ENF samples are presented in Fig. 8. The Al-O-Si vibration band at 548 cm^{-1}, the Al_2OH bending band at 957 cm^{-1} and the Si-O stretching band at 1031 cm^{-1} show reasonable contribution addition of HNTs (as seen in Fig. 8b and c) [6]. Moreover, especially with the increasing aging time, it is seen that there is a notable

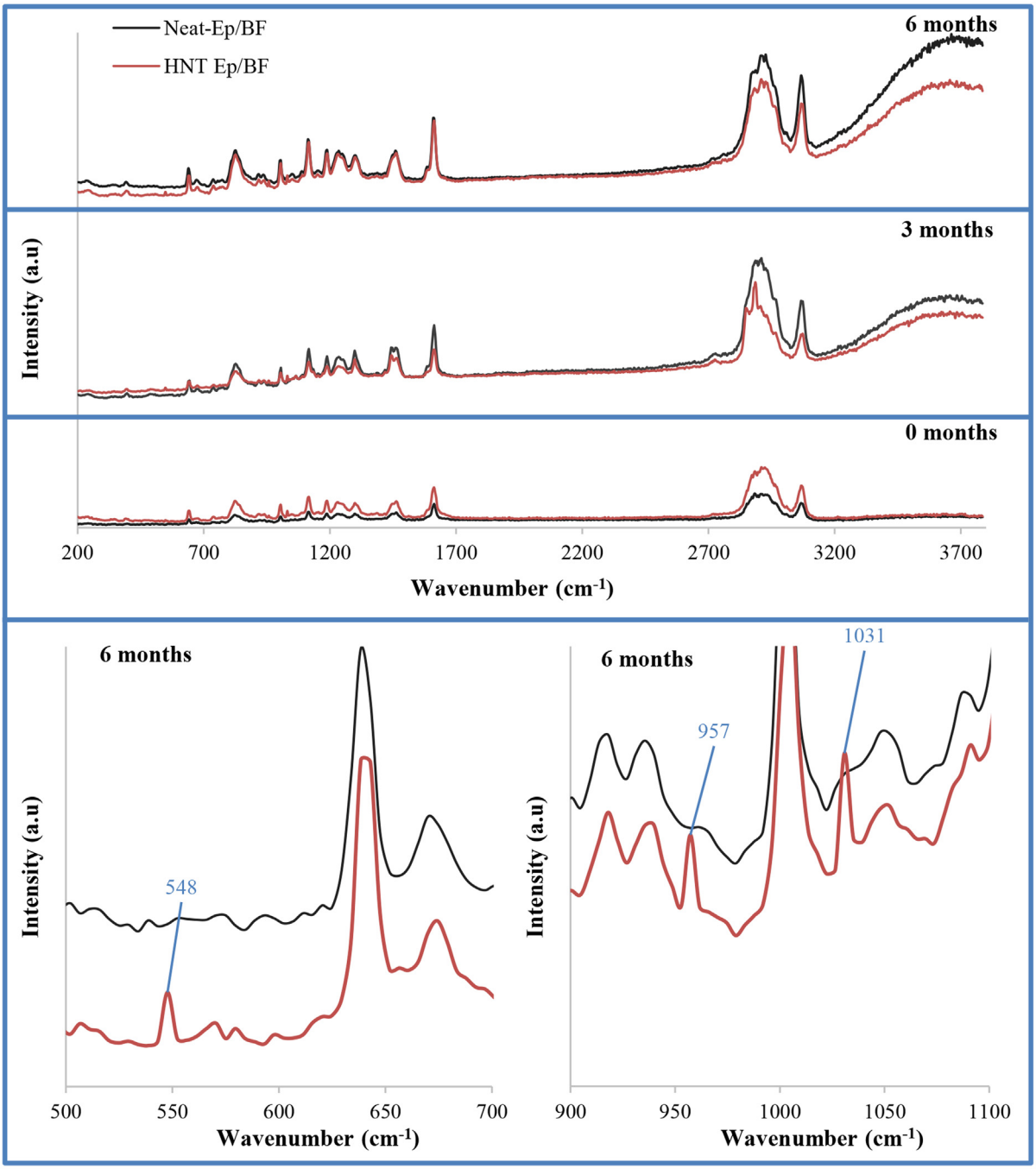

Fig. 8. Raman spectra of the neat and HNT modified multi-scale composite.

increase in the stretching vibrations of hydroxyl groups around the 3650 cm^{-1} wavenumbers for the neat composite samples. It is well known that epoxy water absorption is relevant to the intensity of the hydroxyl group peak [23]. It is seen that the hydroxyl group peak intensity of multi-scale composites is lower than that of the neat composite. It means that HNTs limit the water absorption into epoxy by slowing the diffusion of water.

4. Conclusion

The present study was designed to determine the impact of seawater aging on the mechanical and dynamic mechanical performance of BF/EP composites. Experiments have demonstrated that the mechanical properties are affected considerably by seawater aging. However, the empirical findings illustrate matrix modification with halloysite nanotubes significantly minimized the adverse effect of seawater on durability. After immersed in seawater for 6 months, the shear strength and G_{II} fracture energy values of neat BF/EP samples decline more severe than HNT modified multi-scale composites.

The plasticization effect after seawater aging was manifested by the decreasing glass transition temperature (Tg) according to dynamic mechanical analysis. HNT-basalt/epoxy hybrid nanocomposites evidenced a higher Tg concerning neat basalt/epoxy composites. One of the more significant findings to emerge from this study is that the toughening mechanisms of HNTs such as

pull-out, crack deflection, and crack pinning were attributed to the enhancement in the mechanical performances. The fracture morphology features of multi-scale composites were observed to be rougher than neat counterparts due to the realization of crack path deflections. Additionally, the primary reason for the performance decreasing after seawater immersion was related weakening of the fiber-matrix interfacial bonding. Raman spectra showed that the hydroxyl groups' (OH) peak intensity of neat epoxy specimens more intense compared to the HNT-epoxy samples as the aging time increase. This finding should help to improve predictions of the impact of that the epoxy modifications by adding HNTs decrease seawater uptake.

Declaration of Competing Interest

The authors declare that they have no known competing financial interests or personal relationships that could have appeared to influence the work reported in this paper.

Acknowledgments

The authors would like to thank The Scientific and Technical Research Council of Turkey (TÜBİTAK) (project number:120M369) and Çanakkale Onsekiz Mart University Scientific Research Project Coordination Unit (Project number: FBA-2018-2635) for financial support.

References

[1] I. Panaitescu, T. Koch, V.-M. Archodoulaki, Accelerated aging of a glass fiber/polyurethane composite for automotive applications, Polym. Test. 74 (2019) 245–256.
[2] H. Burak Kaybal, A. Unuvar, Y. Kaynak, A. Avcı, Evaluation of boron nitride nanoparticles on delamination in drilling carbon fiber epoxy nanocomposite materials, J. Compos. Mater. 54 (2) (2020) 215–227.
[3] S. Kasaragadda, I.M. Alarifi, M. Rahimi-Gorji, R. Asmatulu, Investigating the effects of surface superhydrophobicity on moisture ingression of nanofiber-reinforced bio-composite structures, Microsyst. Technol. 26 (2) (2020) 447–459.
[4] T. Liu, X. Liu, P. Feng, A comprehensive review on mechanical properties of pultruded FRP composites subjected to long-term environmental effects, Compos. Part B: Eng. (2020) 107958.
[5] H. Ulus, H.B. Kaybal, V. Eskizeybek, A. Avcı, Enhanced salty water durability of halloysite nanotube reinforced epoxy/basalt fiber hybrid composites, Fibers Polym. 20 (10) (2019) 2184–2199.
[6] H. Ulus, H.B. Kaybal, V. Eskizeybek, A. Avcı, Halloysite nanotube reinforcement endows ameliorated fracture resistance of seawater aged basalt/epoxy composites, J. Compos. Mater. 54 (20) (2020) 2761–2779.
[7] M.Y. Fard, B. Raji, J. Woodward, A. Chattopadhyay, Characterization of interlaminar fracture modes I, II, and I-II of carbon/epoxy composites including in-service related bonding quality conditions, Polym. Test. 77 (2019) 105894, https://doi.org/10.1016/j.polymertesting.2019.05.010.
[8] M. Johar, K.O. Low, H.A. Israr, K.J. Wong, Mode I and mode II delamination of a chopped strand mat E-glass reinforced vinyl ester composite, Plast., Rubber Compos. 47 (9) (2018) 391–397.
[9] P. Hao, I.U. Din, S. Panier, Development of modified arcan fixture for biaxial loading response of fiber-reinforced composites, Polym. Test. 80 (2019) 106148.
[10] A. Mengal, S. Karuppanan, M. Ovinis, In–plane shear properties of basalt–carbon/epoxy hybrid composite laminates: In–plane Schereigenschaften von Basalt-Kohlenstoff/Epoxy-Hybrid-Verbundlaminaten, Materialwiss. Werkstofftech. 48 (3–4) (2017) 261–266.
[11] H. Gu, Dynamic mechanical analysis of the seawater treated glass/polyester composites, Mater. Des. 30 (7) (2009) 2774–2777.
[12] H. Li et al., Effect of seawater ageing with different temperatures and concentrations on static/dynamic mechanical properties of carbon fiber reinforced polymer composites, Compos. B Eng. 173 (2019) 106910.
[13] A. Mlyniec, J. Korta, R. Kudelski, T. Uhl, The influence of the laminate thickness, stacking sequence and thermal aging on the static and dynamic behavior of carbon/epoxy composites, Compos. Struct. 118 (2014) 208–216.
[14] A.P. Costa, E.C. Botelho, L.C. Pardini, Influence of environmental conditioning on the shear behavior of poly (phenylene sulfide)/glass fiber composites, J. Appl. Polym. Sci. 118 (1) (2010) 180–187.
[15] A.M. Figliolini, L.A. Carlsson, Mechanical properties of vinylester resins exposed to marine environments, Polym. Eng. Sci. 53 (11) (2013) 2413–2421.
[16] V. Dhand, G. Mittal, K.Y. Rhee, S.-J. Park, D. Hui, A short review on basalt fiber reinforced polymer composites, Compos. B Eng. 73 (2015) 166–180.
[17] V. Fiore, T. Scalici, G. Di Bella, A. Valenza, A review on basalt fibre and its composites, Compos. B Eng. 74 (2015) 74–94.
[18] A. Abdi, R. Eslami-Farsani, H. Khosravi, Evaluating the mechanical behavior of basalt fibers/epoxy composites containing surface-modified $CaCO_3$ nanoparticles, Fibers Polym. 19 (3) (2018) 635–640.
[19] H. Azizi, R. Eslami-Farsani, Study of mechanical properties of basalt fibers/epoxy composites containing silane-modified nanozirconia, J. Ind. Textiles (2019). 1528083719887530.
[20] M. Bulut et al., Mechanical and dynamic properties of basalt fiber-reinforced composites with nanoclay particles, Arab. J. Sci. Eng. (2019) 1–17.
[21] R.K. Nayak, Influence of seawater aging on mechanical properties of nano-Al2O3 embedded glass fiber reinforced polymer nanocomposites, Constr. Build. Mater. 221 (2019) 12–19.
[22] S. Deng, J. Zhang, L. Ye, J. Wu, Toughening epoxies with halloysite nanotubes, Polymer 49 (23) (2008) 5119–5127.
[23] H. Alamri, I.M. Low, Effect of water absorption on the mechanical properties of nano-filler reinforced epoxy nanocomposites, Mater. Des. 42 (2012) 214–222.
[24] H.B. Kaybal, H. Ulus, V. Eskizeybek, A. Avcı, An experimental study on low velocity impact performance of bolted composite joints part 1: influence of halloysite nanotubes on dynamic loading response, Compos. Struct. 258 (2021) 113415, https://doi.org/10.1016/j.compstruct.2020.113415.
[25] H. Ulus, Ö.S. Şahin, A. Avcı, Enhancement of flexural and shear properties of carbon fiber/epoxy hybrid nanocomposites by boron nitride nano particles and carbon nano tube modification, Fibers Polym. 16 (12) (2015) 2627–2635.
[26] M. Liu, Z. Jia, D. Jia, C. Zhou, Recent advance in research on halloysite nanotubes-polymer nanocomposite, Prog. Polym. Sci. 39 (8) (2014) 1498–1525.
[27] Y. Zhao, W. Liu, L.K. Seah, G.B. Chai, Delamination growth behavior of a woven E-glass/bismaleimide composite in seawater environment, Compos. B Eng. 106 (2016) 332–343.
[28] V. Prasad et al., Enhancing Mode I and Mode II interlaminar fracture toughness of flax fibre reinforced epoxy composites with nano TiO2, Compos. A Appl. Sci. Manuf. 124 (2019) 105505.
[29] M. Liu, B. Guo, M. Du, X. Cai, D. Jia, Properties of halloysite nanotube–epoxy resin hybrids and the interfacial reactions in the systems, Nanotechnology 18 (45) (2007) 455703, https://doi.org/10.1088/0957-4484/18/45/455703.
[30] S. Srivastava, A. Pandey, Mechanical behavior and thermal stability of ultrasonically synthesized halloysite-epoxy composite, Compos. Commun. 11 (2019) 39–44.
[31] Y. Ye, H. Chen, J. Wu, C.M. Chan, Interlaminar properties of carbon fiber composites with halloysite nanotube-toughened epoxy matrix, Compos. Sci. Technol. 71 (5) (2011) 717–723.
[32] J.-K. Kim, M.-L. Sham, Impact and delamination failure of woven-fabric composites, Compos. Sci. Technol. 60 (5) (2000) 745–761.
[33] M.D. Banea, L.F.M. da Silva, R.D.S.G. Campilho, Mode II fracture toughness of adhesively bonded joints as a function of temperature: experimental and numerical study, J. Adhesion 88 (4-6) (2012) 534–551.
[34] Y. Ye, H. Chen, J. Wu, C.M. Chan, Evaluation on the thermal and mechanical properties of HNT-toughened epoxy/carbon fibre composites, Compos. B Eng. 42 (8) (2011) 2145–2150.
[35] J. Militký, A. Jabbar, Comparative evaluation of fiber treatments on the creep behavior of jute/green epoxy composites, Compos. B Eng. 80 (2015) 361–368.
[36] S.H. Lim, K.Y. Zeng, C.B. He, Morphology, tensile and fracture characteristics of epoxy-alumina nanocomposites, Mater. Sci. Eng., A 527 (21-22) (2010) 5670–5676.